Anal. Chem. **2002,** *74,* 1157−1164

In Situ FT-IR Measurements of Competitive Vapor Adsorption into Porous Thin Films Containing Silica Nanoparticles

Charles R. Evans, Tighe A. Spurlin, and Brian L. Frey*

Department of Chemistry, Lake Forest College, 555 North Sheridan Road, Lake Forest, Illinois 60045-2399

Vapor adsorption into porous ultrathin films on a gold surface is investigated with in situ surface plasmon resonance (SPR) and polarization-modulation infrared reflection−absorption spectroscopy (PM-IRRAS). The thin films are prepared by the electrostatic self-assembly of oppositely charged poly(L-lysine) (PL) and silica nanoparticles on a chemically modified gold surface. Characterization with ex situ SPR and PM-IRRAS demonstrates the buildup of multiple PL/SiO_2 bilayers as well as an excellent correlation between the quantitative results from these two techniques. In situ vapor adsorption experiments with these thin films show evidence of porosity, reproducibility, and rapid reversibility. Exposure to acetone vapor ($P/P_0 = 0.032$) causes the film to adsorb 9% acetone by volume, which corresponds to coverage of approximately one-half of the silica nanoparticle surface area. In situ PM-IRRAS provides much information about the molecular interactions occurring in the film upon adsorption or desorption of vapors. Dosing with a mixture of vapors leads to a competition for adsorption into the film, and PM-IRRAS results show that acetone slightly outcompetes nitromethane. These experiments with nanoparticle thin films demonstrate the advantages of using in situ PM-IRRAS for studying reversible adsorption in the presence of vapor mixtures.

Understanding adsorption of chemical species from the vapor or gas phase onto solid surfaces is crucial to many fields. Real-world applications usually entail exposure of a surface to a mixture, but most of the characterization to date has been simplified to one vapor (or gas) at a time. Investigating adsorption from a mixture is important, because unforeseen cooperativity, positive or negative, between different vapors will likely produce erroneous results in many applications. Chemical sensors often must operate in mixtures, and it is not possible to achieve complete selectivity for one vapor while maintaining reversibility, which is a necessity for concentration monitoring. Separation by gas chromatography inherently involves mixtures, yet there are few detailed studies of multicomponent competitive adsorption.[1] Studies of pollutant partitioning to aerosol or soil particles in the natural environment deal with the complex mixture called air. Even industrial applications such as catalysis and chemical vapor deposition often require simultaneous exposure to more than one vapor. In all of these fields, ultrathin films serve as model systems as well as current or future applications. Therefore, we need a characterization technique for ultrathin films that is amenable to vapor mixtures. Unfortunately, most in situ measurements of adsorption have involved nonselective optical or mass sensing techniques that lack chemical specificity, which confines them to single vapor experiments. In this paper, we present polarization-modulation infrared reflection−absorption spectroscopy (PM-IRRAS) for studies of competitive vapor adsorption into ultrathin films on metal surfaces.

PM-IRRAS eliminates vapor-phase absorptions from the spectra, thereby making it ideal for in situ measurements.[2−5] Ex situ IRRAS, with or without polarization-modulation, is a standard method for providing information about composition, order, orientation, and chemical interactions on a surface or within a thin film.[6−11] Frequently, researchers switch from infrared spectroscopy to a more sensitive technique with greater surface-selectivity for monitoring in situ adsorption (e.g., quartz crystal microbalance, surface acoustic wave devices, surface plasmon resonance, or various other optical methods). However, these methods cannot identify adsorbates; they merely quantify them. Thus, vibrational spectroscopy has an advantage, but its surface-selectivity must be enhanced. Crooks and co-workers have performed a number of excellent vapor adsorption studies with conventional IRRAS[12−14] and one with PM-IRRAS,[15] but in many cases, they looked at species remaining on the surface after

(1) Zhu, C.; Yun, K. S.; Parcher, J. F. *Anal. Chem.* **1995**, *67*, 1596−1602.

(2) Frey, B. L.; Corn, R. M.; Weibel, S. C. In *Handbook of Vibrational Spectroscopy*; Chalmers, John M., Griffiths, Peter R., Eds.; John Wiley & Sons: Chichester, 2001; Vol. 2, in press.

(3) Golden, W. G.; Dunn, D. S.; Overend, J. *J. Phys. Chem.* **1978**, *82*, 843−844.

(4) Dowrey, A. E.; Marcott, C. *Appl. Spectrosc.* **1982**, *36*, 414−416.

(5) Faguy, P. W.; Richmond, W. N.; Jackson, R. S.; Weibel, S. C.; Ball, G.; Payer, J. H. *Appl. Spectrosc.* **1998**, *52*, 557−564.

(6) Umemura, J. In *Handbook of Vibrational Spectroscopy*; Chalmers, J. M.; Griffiths, P. R., Eds.; John Wiley & Sons: Chichester, 2001; Vol. 2, in press.

(7) Porter, M. D. *Anal. Chem.* **1988**, *60*, 1143A−1155A.

(8) Nuzzo, R. G.; Dubois, L. H.; Allara, D. L. *J. Am. Chem. Soc.* **1990**, *112*, 558−569.

(9) Crooks, R. M.; Sun, L.; Xu, C.; Hill, S. L.; Ricco, A. J. *Spectroscopy* **1993**, *8*, 28.

(10) Frey, B. L.; Hanken, D. G.; Corn, R. M. *Langmuir* **1993**, *9*, 1815−1820.

(11) Shon, Y.-S.; Colorado, R. J.; Williams, C. T.; Bain, C. D.; Lee, T. R. *Langmuir* **2000**, *16*, 541−548.

(12) Xu, C.; Sun, L.; Kepley, L. J.; Crooks, R. M. *Anal. Chem.* **1993**, *65*, 2102−2107.

(13) Yang, H. C.; Dermondy, D. L.; Xu, C.; Ricco, A. J.; Crooks, R. M. *Langmuir* **1996**, *12*, 726−735.

(14) Wells, M.; Dermody, D. L.; Yang, H. C.; Kim, T.; Crooks, R. M. *Langmuir* **1996**, *12*, 1989−1996.

10.1021/ac010990m CCC: $22.00
Published on Web 01/25/2002

removal of the vapor-phase probe molecules. A couple researchers have acquired in situ spectra by subtracting an s-polarized spectrum from a p-polarized IRRAS spectrum to remove vapor-phase peaks.[16−18] PM-IRRAS employs this same strategy, but the 74 kHz modulation between p and s polarizations improves the cancellation of bulk-phase absorptions. The PM approach aided Faguy et al. in studying the buildup of corrosion products and entrained water on copper surfaces exposed to acidic gases and water vapor.[5] The present PM-IRRAS study differs not only in the type of ultrathin film, but also because it is an investigation of a rapidly reversible vapor adsorption.

Before characterizing the vapor adsorption properties of ultrathin films, they must first be prepared. On metal surfaces, ultrathin films have been prepared with numerous substances by several methods to achieve vastly different properties.[19,20] One facile and often used method is electrostatic self-assembly (ESA), whereby alternating layers of oppositely charged substances are deposited onto a surface layer-by-layer.[21,22] ESA has been employed most frequently for polymer films but also for films incorporating nano-objects such as clay platelets and supramolecular complexes, as well as metallic, semiconducting, or insulating nanoparticles.[22−24] More specifically, ultrathin films containing charged silica nanoparticles and an oppositely charged polymer have been created both on planar metal surfaces and on colloidal latex spheres.[25−28] Lvov et al. reported that such films contain a void volume that was not filled with water,[27] and therefore, we expect vapors to adsorb into these films, although it has not previously been demonstrated. Adsorption onto silica surfaces, in general, has been widely studied because of its notable application in chromatography, but also in environmental studies of pollutant partitioning and transport in soils.[1,29−32] Furthermore, ultrathin films of silica nanoparticles have potential applications in chemical sensing and separations. Thus, they provide a system of substantial interest for demonstrating the utility of our in situ characterization techniques.

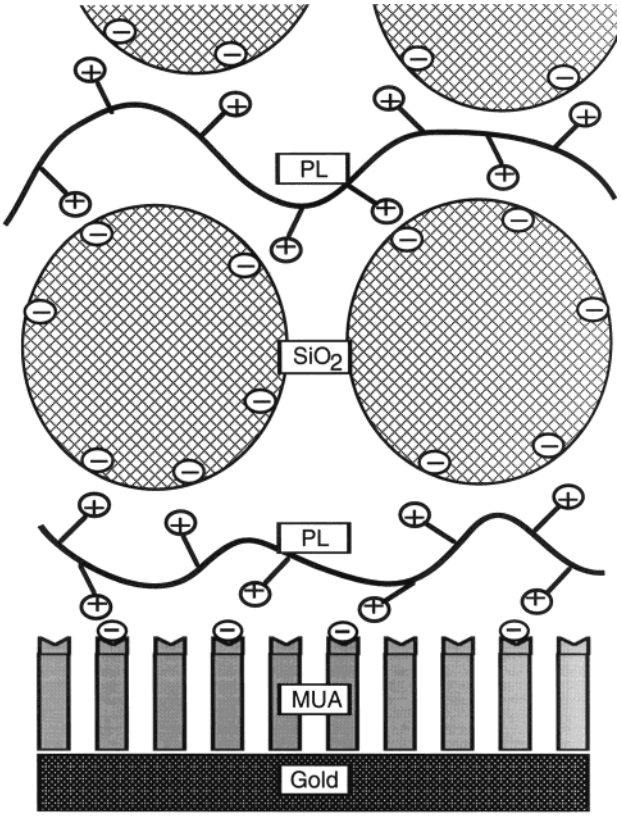

Figure 1. Schematic diagram showing a thin film composed of positively charged poly(L-lysine) (PL) and negatively charged silica nanoparticles (SiO_2) deposited via electrostatic assembly on top of a MUA-modified gold surface. The layer-by-layer approach allows a variable number of PL/SiO_2 bilayers. Not to scale, and some small counterions are omitted for clarity.

In this paper, we report the preparation, characterization and vapor adsorption properties of multilayer thin films formed from poly-L-lysine (PL) and silica nanoparticles, as depicted in Figure 1. The layer-by-layer approach of ESA is used to create films with a variable number of PL/SiO_2 bilayers, and they are characterized with ex situ PM-IRRAS and surface plasmon resonance (SPR) thickness measurements.[33−35] Reversible vapor adsorption into these porous PL/SiO_2 films is examined with in situ PM-IRRAS but also with in situ SPR. The SPR data verify the quantitative nature of our infrared measurements as well as provide absolute quantification. Of course, SPR is one of those nonselective techniques limited to a single vapor at a time. Therefore, PM-IRRAS is employed to determine the relative amounts of adsorption for each vapor from a mixture. This work represents one of a few in situ investigations of competitive vapor adsorption and the first involving porous ultrathin films containing nanoparticles.

EXPERIMENTAL SECTION

Materials. (3-Mercaptopropyl)trimethoxysilane (MPS) [Aldrich], 11-mercaptoundecanoic acid (MUA) [Aldrich], poly(L-lysine) hydrobromide (PL) [MW 9400, Sigma], LUDOX AS-30 colloidal

(15) Crooks, R. M.; Yang, H. C.; McEllistrem, L. J.; Thomas, R. C.; Ricco, A. J. *Faraday Discuss.* **1997**, *107*, 285−305.
(16) Hierlemann, A.; Ricco, A. J.; Bodenhofer, K.; Gopel, W. *Anal. Chem.* **1999**, *71*, 3022−3035.
(17) Bertilsson, L.; Potje-Kamloth, K.; Liess, H.-D.; Liedberg, B. *Langmuir* **1999**, *15*, 1128−1135.
(18) Bertilsson, L.; Potje-Kamloth, K.; Liess, H.-D.; Engquist, I.; Liedberg, B. *J. Phys. Chem. B* **1998**, *102*, 1260−1269.
(19) Ulman, A. *Chem. Rev.* **1996**, *96*, 1533−1554.
(20) Dubois, L. H.; Nuzzo, R. G. *Annu. Rev. Phys. Chem.* **1992**, *43*, 437−463.
(21) Decher, G. *Science* **1997**, *277*, 1232−1237.
(22) Bertrand, P.; Jonas, A.; Laschewsky, A.; Legras, R. *Macromol. Rapid Commun.* **2000**, *21*, 319−348.
(23) Laschewsky, A.; Wischerhoff, E.; Kauranen, M.; Persoons, A. *Macromolecules* **1997**, *30*, 8304−8309.
(24) Fendler, J. H. *Chem. Mater.* **1996**, *8*, 1616−1624.
(25) Caruso, F.; Lichtenfeld, H.; Giersig, M.; Mohwald, H. *J. Am. Chem. Soc.* **1998**, *120*, 8523−8524.
(26) Caruso, F.; Mohwald, H. *Langmuir* **1999**, *15*, 8276−8281.
(27) Lvov, Y.; Ariga, K.; Onda, M.; Ishinose, I.; Kunitake, T. *Langmuir* **1997**, *13*, 6195−6203.
(28) Nelson, B. P.; Frutos, A. G.; Brockman, J. M.; Corn, R. M. *Anal. Chem.* **1999**, *71*, 3928−3934.
(29) Vansant, E. F.; Van Der Voort, P.; Vrancken, K. C. *Characterization and Chemical Modification of the Silica Surface*; Elsevier: New York, 1995.
(30) Ringwald, S. C.; Pemberton, J. E. *Environ. Sci. Technol.* **2000**, *34*, 259−265.
(31) Goss, K.-U. *Environ. Sci. Technol.* **1992**, *26*, 2287−2294.
(32) Rivera, D.; Harris, J. M. *Anal. Chem.* **2001**, *73*, 411−423.
(33) Frutos, A. G.; Corn, R. M. *Anal. Chem.* **1998**, *70*, 449A−455A.
(34) Knoll, W. *Annu. Rev. Phys. Chem.* **1998**, *49*, 569−638.
(35) Hanken, D. G.; Jordan, C. E.; Frey, B. L.; Corn, R. M. *Electroanal. Chem.* **1998**, *20*, 141−225.

silica (12 nm diam) [Dupont via Aldrich], boric acid [Fluka], sodium hydroxide [Fluka], and absolute ethanol [Aaper] were used as received. Spectrophotometric grade acetone [Aldrich] and puriss grade nitromethane [Fluka] were dried over 3A and 4A molecular sieves [Aldrich], respectively. Nanopure filtered water (18 MΩ) from a Barnstead system was used throughout. All plastic tubing was either 890 FEP or plasticizer-free silicone [VWR Scientific].

Formation of PL/SiO_2 Thin Films. Thin gold films (50 nm) were vapor-deposited onto BK-7 microscope cover glasses (no. 1.5, 18 × 18 mm) that had been silanized with MPS as described previously.[36,37] The freshly vapor-deposited gold slides were placed into 1 mM ethanolic solutions of MUA for at least 18 h before they were thoroughly rinsed with ethanol and then water. The PL and SiO_2 layers were formed by alternating 20 min immersions in (i) a 0.2 mg/mL PL in 50 mM borate buffer solution at pH 8.8 and (ii) a 25 mg/mL aqueous suspension of the LUDOX colloidal silica at pH 9.1. Thorough rinsing with water was performed upon emersion from each solution. Unless otherwise indicated, the samples mentioned in this paper consisted of three PL/SiO_2 bilayers atop a MUA monolayer.

Two other sources of colloidal silica were investigated: (i) Snowtex-40 colloidal silica at pH 10.1 [Nissan Chemical Industries], and (ii) a base-hydrolyzed silica sol at pH 8.8 prepared via the sol−gel method by the Anderson group, as described elsewhere.[38] Both acted very similarly to the LUDOX AS-30 in terms of layer formation and vapor adsorption properties. The only difference was the layer thickness caused by different particle size and degree of aggregation.

Surface Plasmon Resonance (SPR) Measurements. An angle-scanning SPR instrument was assembled from a HeNe laser (2 mW at 632.8 nm, Newport), a calcite polarizer (Melles Griot) for selecting p-polarized light, a focusing lens, a sample assembly, a collection lens, and a photodiode detector (Thor Labs DET110). The sample assembly consisted of a 25-mm-diameter BK7 glass hemispherical prism (Harold Johnson Optical Labs) mounted on a micrometer-driven rotation stage (Oriel). Optical contact between a sample and the prism was achieved with a thin layer of ethylene glycol. The combination of the focusing lens and the prism yielded collimated light on the gold surface. The incident angle was scanned by a computer-controlled stepper motor turning the rotation stage micrometer with a precision of 0.004° per step; the collection lens and detector were rotated at twice the angle of the sample in order to collect the reflected light. The laser beam was mechanically chopped at 380 Hz (Thor Labs MC1000), and the detector output was demodulated by a lock-in amplifier (Thor Labs LIA100) before being recorded by a computer.

This angle-scanning SPR instrument yielded reflectivity versus incident angle curves that were fitted with complex Fresnel calculations to determine the thickness of adsorbed layers, as discussed previously.[39] These calculations assume a uniform layer with a certain index of refraction (n), but our films are actually intermingled PL ($n = 1.52$) and silica ($n = 1.46$), with air ($n = 1.00$) as well. Thus, a weighted average index of refraction of 1.35 was estimated from 63% silica (volume ratio occupied by hexagonally close-packed spheres), 12% PL (numerous SPR measurements determined that our films contain about one-fifth as much PL as silica), and the remaining 25% being air (Lvov et al. showed that the interstitial spaces were not filled with water[27]). This estimate of $n = 1.35$ is reasonable, and an error of 0.05 in n produces only a 7% error in absolute thickness and much less in relative comparisons.[39] Therefore, SPR measurements provide an excellent quantitative measure of the amount of material adsorbed to the surface.

The in situ SPR measurements required a sample assembly that included an in situ cell machined from delrin with a cell volume of 2 mL and sealed to the gold surface using a Viton O-ring. In addition to the angle-scanning measurements, some of the in situ SPR experiments were performed at a fixed angle of incidence, as explained in the Results and Discussion section.

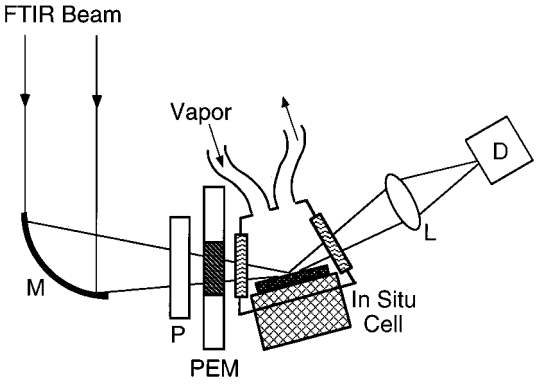

Figure 2. Optical layout of the in situ PM-IRRAS apparatus. The infrared beam is focused with a parabolic mirror (M), sent through a polarizer (P) and photoelastic modulator (PEM), reflected off the sample, collected by a lens (L), and detected by a detector (D). The sample, a thin film on a gold surface, sits inside the in situ cell that allows dosing with various vapors or purging with nitrogen gas.

PM-IRRAS Measurements. The optical layout of the PM-IRRAS instrument is shown in Figure 2. The infrared beam from an FT-IR spectrometer (Mattson Polaris) was focused using a 6-in. focal length off-axis parabolic mirror (Janos Technology) at an incident angle of 77° onto the gold samples mounted inside an in situ cell having BaF_2 windows, Viton O-ring seals, and a cell volume of 30 mL. The light was first polarized with a ZnSe wire-grid polarizer (Reflex Analytical), and then the polarization was modulated at 74 kHz using a photoelastic modulator (Hinds PEM-90). The light reflected from the sample was collected with a ZnSe lens and focused onto a narrow band HgCdTe detector (Madison Instruments). A synchronous sampling demodulator (GWC Instruments) was used to demodulate the polarization-dependent signal into a sum signal ($I_p + I_s$) and a difference signal ($I_p - I_s$) where I_p and I_s refer to the intensity of p and s-polarized light, respectively. A block average of 500 scans at 4 cm^{-1} resolution was recorded in 10 blocks of 50 difference signal scans and only 8 sum signal scans; less noise in the sum signal allowed fewer scans and reduced the acquisition time. Ratioing the difference signal to the sum signal yielded a transmittance spectrum with upward going peaks on a broadly curving baseline, which results from the relative efficiency of the PEM at different wavelengths. These transmittance spectra were normalized to

(36) Goss, C. A.; Charych, D. H.; Majda, M. *Anal. Chem.* **1991**, *63*, 85−88.
(37) Frey, B. L.; Corn, R. M. *Anal. Chem.* **1996**, *68*, 3187−3193.
(38) Chu, L.; Anderson, M. A. *J. Membr. Sci.* **1996**, *110*, 141−149.
(39) Jordan, C. E.; Frey, B. L.; Kornguth, S.; Corn, R. M. *Langmuir* **1994**, *10*, 3642−3648.

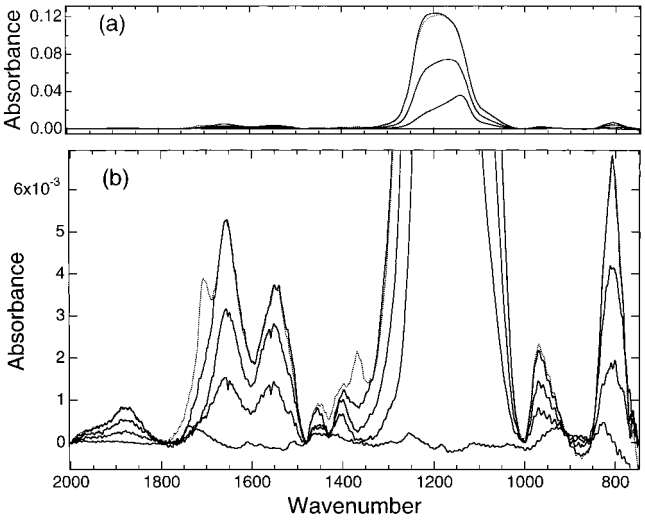

Figure 3. PM-IRRAS spectra showing the buildup of a PL/SiO_2 thin film, where part b is a vertically expanded version of part a in order to show peaks other than the very large asymmetric Si−O−Si stretching peak. The four solid line spectra correspond to 0, 1, 2, and 3 PL/SiO_2 bilayers and show the gradual increase of both PL and SiO_2 bands (0 bilayers is simply a MUA-modified gold surface). The dotted line spectrum is an in situ spectrum of the 3 bilayer film exposed to acetone vapor and will be discussed later.

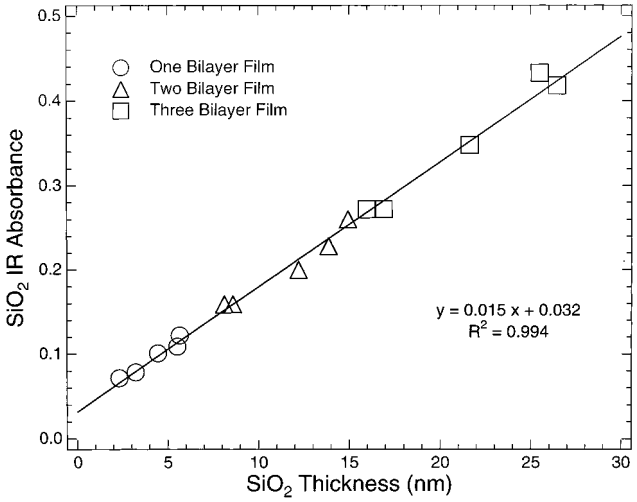

Figure 4. A correlation plot between the IR absorbance of the ν_{as}Si−O−Si band and the SPR-measured thickness of silica in the thin film. Five different samples are represented by these data, which were taken after the first bilayer (circles), the second bilayer (triangles), and the third bilayer (squares). One trend is that a smaller first layer results in smaller second and third layers as well (e.g., the lowest two circles correspond to the same samples that gave the lowest two triangles and squares). An excellent linear correlation is observed between the PM-IRRAS and SPR data.

remove this broadly curving baseline and were converted to absorbance units, as discussed elsewhere.[2]

In Situ Measurements. In situ cells for both instruments were purged with high-purity nitrogen gas (Air Products). Vapors of a certain concentration were prepared in 2-L Teflon gas sampling bags having a polypropylene valve with a small septum beside it (Alltech). For example, a bag of acetone vapor ($P/P_0 = 0.016$, $P_0 = 760$ mmHg) was prepared by (i) half-filling a bag with N_2, (ii) injecting 100 μL of dried acetone through the septum, (iii) allowing the acetone to completely evaporate, and (iv) filling the bag to 2.0 L with N_2. The vapor was pumped into either of the in situ cells through some tubing by applying gentle pressure to the bag.

RESULTS AND DISCUSSION

Characterization of PL/SiO_2 Thin Films. The PL/SiO_2 thin films were prepared using electrostatic layer-by-layer assembly of oppositely charged polymers and nanoparticles (see Figure 1). First, a self-assembled monolayer of 11-mercaptoundecanoic acid (MUA) was formed on a gold surface, followed by immersion into an aqueous poly(L-lysine) solution buffered to pH 8.8. Deprotonation of MUA molecules at this pH allowed for the electrostatic adsorption of a monolayer of PL. Subsequent immersion into a colloidal silica suspension at the similar pH of 9.1 yielded a layer of negatively charged silica nanoparticles atop the positively charged PL monolayer. Additional PL/SiO_2 bilayers were easily added by alternate exposure to the PL and silica solutions, creating a film of variable thickness.

PM-IRRAS spectra representing the sequential buildup of three PL/SiO_2 bilayers are shown in Figure 3. The MUA spectrum contains the well-documented 1738 cm^{-1} carbonyl stretching band of the protonated carboxylic acid groups. This band largely disappears after PL adsorption as a result of deprotonation and generation of carboxylate-ammonium ion pairs.[39] The spectra representing 1, 2, and 3 bilayers show peaks due to both PL and the silica nanoparticles. The amide I and amide II bands of PL occur at 1658 and 1550 cm^{-1}, respectively, along with a couple of smaller PL peaks at 1458 and 1400 cm^{-1}. The silica nanoparticles give bands at 1880 cm^{-1} (skeleton overtone), 1220/1130 cm^{-1} (ν_{as}Si−O−Si), 970 cm^{-1} (νSi−OH···H_2O), and 808 cm^{-1} (ν_sSi−O−Si).[29,40−43] Thus, the PM-IRRAS spectra verify the assembly of multiple bilayers of PL and silica nanoparticles onto the MUA-modified gold surface.

The IR absorbance of the large asymmetric Si−O−Si stretching band shows a correlation to the SPR-measured film thickness, as seen in Figure 4. SPR measurements were performed using an angle-scanning setup, and the raw data were converted to absolute thicknesses using a film index of refraction of 1.35, as explained in the Experimental Section. The layer thickness data in Figure 4 represent only the SiO_2 portion of the film (the PL contribution was subtracted), because the IR absorbance of the Si−O−Si stretching band is due solely to silica. Since the spherical silica nanoparticles cannot have any preferential orientation on the surface, as occurs with some SAMs, the IR absorbance should depend solely on the amount adsorbed. The correlation coefficient of 0.994 demonstrates excellent agreement between the SPR and PM-IRRAS measurements and, thereby, corroborates the linearly quantitative nature of both techniques.

The SiO_2 layer thickness is somewhat small at first, but it reaches a consistent and expected thickness after a couple layers. As seen in Figure 4, the first layer was always the thinnest at 4

(40) Morrow, B. A.; Gay, I. D. *Surfactant Sci. Ser.* **2000**, *90*, 9−33.
(41) Brinker, C. J.; Scherer, G. W. *Sol−Gel Science: The Physics and Chemistry of Sol−Gel Processing*; Academic Press: Boston, 1990.
(42) Jones, S. D.; Pritchard, T. N.; Lander, D. F. *Microporous Mater.* **1995**, *3*, 419−431.
(43) Lin-Vien, D.; Colthup, N. B.; Fateley, W. G.; Grasselli, J. G. *The Handbook of Infrared and Raman Characteristic Frequencies of Organic Molecules*; Academic Press: Boston, 1991.

nm (average); the second one gave an additional thickness of 7 nm; and the third one, an additional 10 nm. Subsequent layers yielded ~10−15 nm per layer (data not shown in Figure 4 because IR absorbances greater than 0.5 are not necessarily linear). Some other researchers have also noticed a nonlinear buildup during the initial few layers of electrostatic self-assembly.[23,44] This so-called induction period is sometimes required before achieving a uniformly charged surface upon each emersion from polyelectrolyte solution.[44] One possible remedy employs a precursor layer of alternately charged polymers before commencing with the silica nanoparticles.[26,27] However, after the induction period, our eventual layer thickness of 10−15 nm is in accord with the 12-nm diameter of these silica nanoparticles, indicating essentially complete monolayers.

A full layer of nanoparticles still allows for porosity in the film, because even close-packed spheres have interstitial spaces. Certainly the polycation accounts for some of the space between nanoparticles, but it does not completely fill those spaces, as shown by Lvov et al.[27] and by the estimation of 25% porosity given in the Experimental Section. Our three-bilayer films might have even greater porosity, since the first couple layers do not contain a close-packed array of silica nanoparticles. Regardless of the exact amount of air space in the PL/SiO_2 thin films, their porous nature is affirmed and exploited by the reversible vapor adsorption experiments reported in the next section.

Single Vapor Adsorption/Desorption Experiments. After thin films of PL/SiO_2 were prepared, their vapor adsorption properties were investigated using volatile organic compounds utilizing the in situ capabilities of PM-IRRAS and SPR. As discussed previously, the solid line spectra in Figure 3 show the ex situ buildup of a three-bilayer sample. The dotted line spectrum in the figure, however, represents an in situ spectrum obtained during exposure of this sample to acetone vapor ($P/P_0 = 0.016$) in nitrogen gas. The spectral changes caused by the acetone vapor are most easily observed with a difference spectrum, such as the one shown in Figure 5.

For this in situ measurement, we must prove that the bands in the PM-IRRAS spectrum arise from acetone adsorbed into the PL/SiO_2 thin film, as opposed to that in the bulk vapor-phase. The position of the carbonyl band at 1708 cm^{-1} indeed indicates adsorbed acetone rather than vapor-phase acetone, which has its peak at 1738 cm^{-1}. Furthermore, bulk acetone in the liquid phase yields a peak at 1716 cm^{-1}, and so the shift to 1708 cm^{-1} suggests the π electrons in the carbonyl group are interacting with hydrogen bonding donor sites (e.g., Si−O−H) at the surface of the silica nanoparticles.[45] The carbonyl band in Figure 5 does have a tail on the high frequency side, which arguably could represent vapor-phase acetone incompletely canceled by the PM-IRRAS technique. However, a control experiment refutes that conclusion. The dotted line difference spectrum was obtained with the same in situ acetone vapor concentration but using a sample having only MUA and PL monolayers without any silica. It shows only a tiny acetone band occurring at 1720 cm^{-1}, again indicating a condensed state, and it is not unexpected that some acetone would adsorb to the MUA/PL surface. All of this evidence, along with the absence of any atmospheric water vapor peaks proves that PM-IRRAS completely eliminates signals due to bulk phase species, and therefore, it is an excellent technique for studying reversible in situ adsorption.

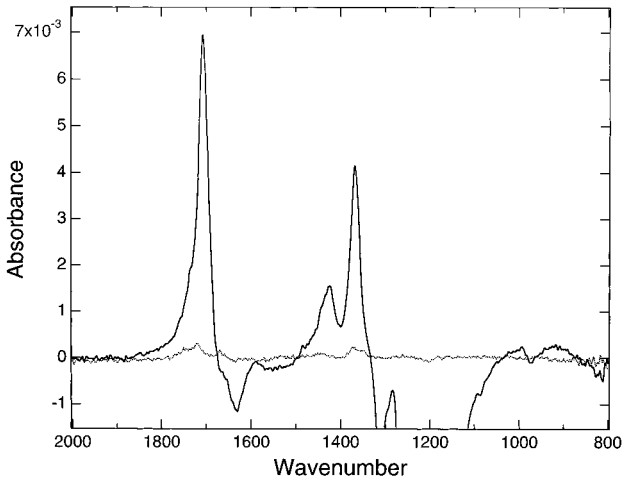

Figure 5. Difference spectra demonstrating acetone adsorption into a PL/SiO_2 thin film. The difference spectrum results from subtracting two PM-IRRAS spectra, the one obtained in the presence of acetone vapor minus the one obtained in nitrogen gas. In the solid line spectrum, notice the positive peaks due to acetone at 1708, 1425, and 1368 cm^{-1}. The negative-going peak from 1300 to 1100 cm^{-1} results from relatively small changes in the huge ν_{as}Si−O−Si band and has been cut off in this spectrum to better show the acetone bands. The dotted line spectrum represents a control experiment as explained in the text.

Having observed that acetone vapor adsorbs to the silica thin film, an absolute quantity of adsorbed acetone was determined from SPR measurements. Figure 6a shows the results of angle-scanning SPR measurements for a PL/SiO_2 thin film in the presence of laboratory air, nitrogen, and finally, acetone vapor. The angle of minimum reflectivity, called the SPR angle, started at 47.37° in air and then, upon exposure to nitrogen, shifted "backward" by about 0.17°, suggesting a desorption process (discussed below). Subsequent exposure to acetone vapor ($P/P_0 = 0.032$) shifted the SPR angle "forward" by 0.30°, which corresponds to an acetone layer thickness of 1.8 nm (assuming $n = 1.36$, the value for bulk acetone). This result is much larger than the molecular dimension of acetone (ca. 0.5 nm), and therefore, it suggests adsorption into a porous film rather than only onto the outer surface of the film. Further evidence of porosity includes the fact that substantially more acetone adsorption occurs with thicker PL/SiO_2 films, such as those having more bilayers. For instance, a controlled experiment involving one, two, and three bilayer films, having thicknesses of 7.9, 14.6, and 22.5 nm, resulted in acetone adsorption of 1.3, 2.2, and 3.9 nm, respectively. Since the PL/SiO_2 films are porous, it is more appropriate to talk about a change in index of refraction for the thin film as acetone adsorbs and replaces nitrogen gas in the pores. For the sample shown in Figure 6, we have calculated that index of refraction change to be $\Delta n = 0.036$ (i.e., from 1.35 up to 1.386). Recall that $n = 1.35$ was estimated from a weighted average of 63% silica ($n = 1.46$), 12% PL ($n = 1.52$), and 25% nitrogen gas ($n = 1.00$). Now a fourth component, acetone ($n = 1.36$), has replaced some of the nitrogen, and using the new overall $n =$

(44) Advincula, R.; Aust, E.; Meyer, W.; Knoll, W. *Langmuir* **1996**, *12*, 3536−3540.
(45) Rivera, D.; Poston, P. E.; Uibel, R. H.; Harris, J. M. *Anal. Chem.* **2000**, *72*, 1543−1554.

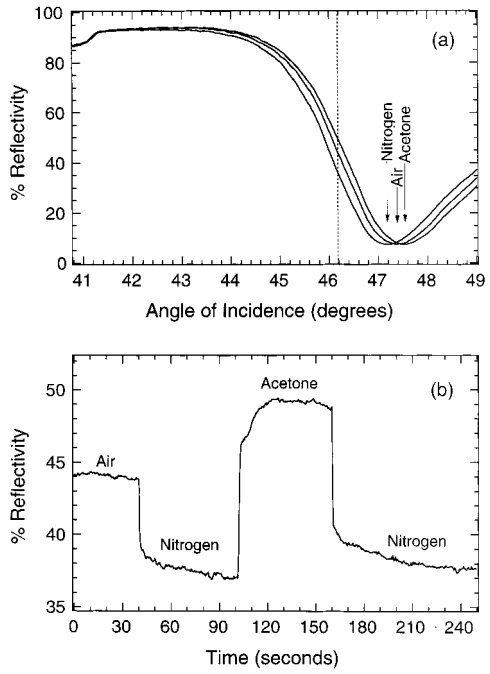

Figure 6. (a) In situ SPR angle-scanning measurements for a three bilayer PL/SiO_2 film (thickness = 22.4 nm). The initial SPR angle of 47.37° (air) shifts to the smaller angle of 47.20° (nitrogen), indicating desorption. Next, a shift to the larger angle of 47.50° demonstrates that acetone is adsorbing into the film. (b) In situ SPR fixed-angle measurement for the same sample and vapors used in part a. Now the percent reflectivity (% *R*) is monitored as a function of time at a fixed angle of 46.18° shown as the dashed line in part a. A decrease or increase of % *R* indicates desorption or adsorption, respectively.

1.386, we calculated that the film contained 9% acetone and 16% nitrogen.

Although 9% acetone in the film is more informative than $\Delta n = 0.036$, we could envision a clearer picture of the film knowing whether this 9% represents a fraction of a monolayer, a monolayer, or multilayers of acetone coating the surfaces of the silica nanoparticles. Assuming a film of 12-nm silica particles comprising 63% (by volume) of the film, the adsorption of 9% acetone to these particles would increase their volume by one-seventh. This volume increase corresponds to a new particle diameter of 12.5 nm or a 0.25 nm layer of acetone all around the nanoparticles. Since an acetone molecule is about 0.5 nm in length, we conclude that about half of the nanoparticle surface area is covered with adsorbed acetone at this concentration ($P/P_0 = 0.032$). This calculation required several assumptions, such as the original composition ratio of the film, no film swelling, and that adsorption occurs only onto the silica rather than PL as well. Nonetheless, the result gives at least a reasonable picture of adsorption occurring into these porous films. SPR measurements have provided an absolute measurement of acetone adsorption into the nanoparticle films whether one prefers to think of it as a thickness of 1.8 nm, a Δn of 0.036, a percent-by-volume of 9%, or one-half of a layer of acetone on all silica nanoparticles.

Another in situ SPR method provides more facile observation of relative amounts of adsorption and desorption (Figure 6b). For this method, the sample was held at a fixed angle of 46.18° (represented by the dashed line in Figure 6a). As the air was replaced with nitrogen, the reflectivity decreased from 44 to 37%,

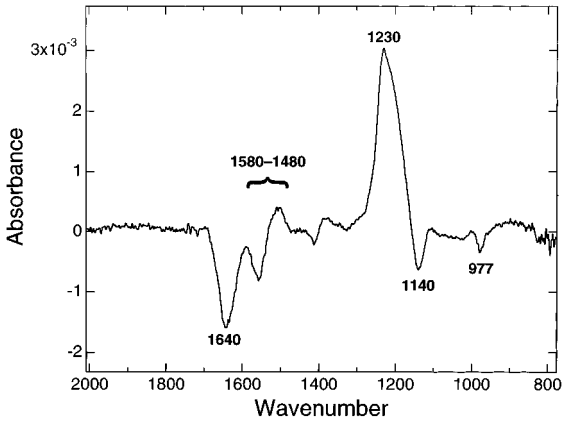

Figure 7. PM-IRRAS difference spectrum showing the dehydration of a PL/SiO2 film when laboratory air was replaced by dry nitrogen gas.

and exposure to acetone vapor caused an increase to 49%. These values correspond well with the reflectivities obtained via the angle-shift measurements shown in part a of the figure, but the fixed-angle method provides a real-time measurement of adsorption that could be used for kinetics studies. A qualitative look at the data in Figure 6b indicates that adsorption (and desorption) to these PL/SiO_2 thin films occurs with a very rapid change followed by a much slower phenomenon. Quantitative kinetics studies, however, have been left to future SPR experiments.

Surface plasmon resonance lacks chemical selectivity, whereas PM-IRRAS easily determines what compound has adsorbed or desorbed from the film. For example, PM-IRRAS showed conclusively (but not surprisingly) that water was desorbing from the thin film upon changing from air to nitrogen. Figure 7 is the difference spectrum between nitrogen and air, and the downward peak at 1640 cm^{-1} (δHOH) demonstrates the loss of adsorbed water. Looking back at Figure 5, a small downward peak at 1630 cm^{-1} indicates that acetone has caused some additional water desorption over that caused by purging with nitrogen. Although interesting, this result is not unexpected when one considers that a nitrogen purge does not lead to complete removal of physisorbed water from silica, which requires heating to at least 373 K.[29,41] A few other reproducible features appear in this dehydration spectrum of Figure 7: (i) a decrease in the band at 977 cm^{-1} (νSi−OH···H_2O), which is expected upon removal of water from the film; (ii) an increase at 1230 cm^{-1} along with a decrease at 1140 cm^{-1}, which probably results from condensation reactions, forming new Si−O−Si bonds at the surface of the silica nanoparticles upon dehydration of the film; and (iii) an interesting derivative-shaped feature from 1580 to 1480 cm^{-1}. We attribute this latter feature to a shift in the amide II band (νC−N and δC−N−H) of polylysine. This shift to lower frequencies occurs upon formation of hydrogen bonds between residues of a polypeptide chain, such as PL.[43,46] Such hydrogen bonding is allowed after the removal of water, which was itself hydrogen bonded to the amide functional groups. A similar shift might be expected for the amide I (νC=O), but it was not observed, although it could be obscured by the 1640 cm^{-1} water band. This dehydration of the film is quite reversible, as evidenced by obtaining a spectrum after dosing the sample with

(46) Jackson, M.; Haris, P. I.; Chapman, D. *Biochim. Biophys. Acta* **1989**, *998*, 75−79.

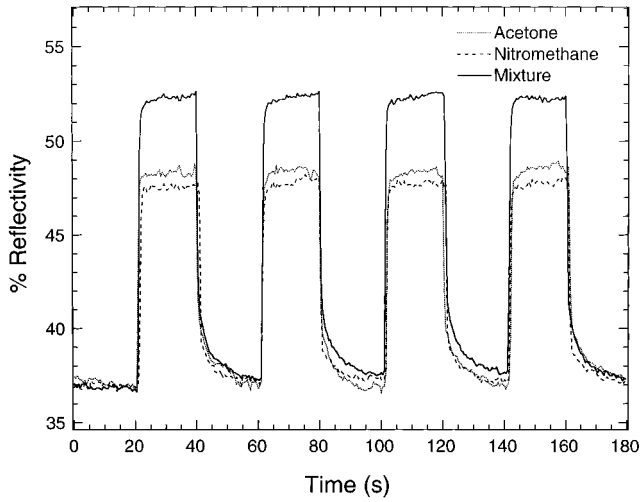

Figure 8. In situ SPR fixed-angle measurements showing four cycles of adsorption and subsequent desorption for three different vapors: acetone (dotted), nitromethane (dashed), and a mixture of the two (solid).

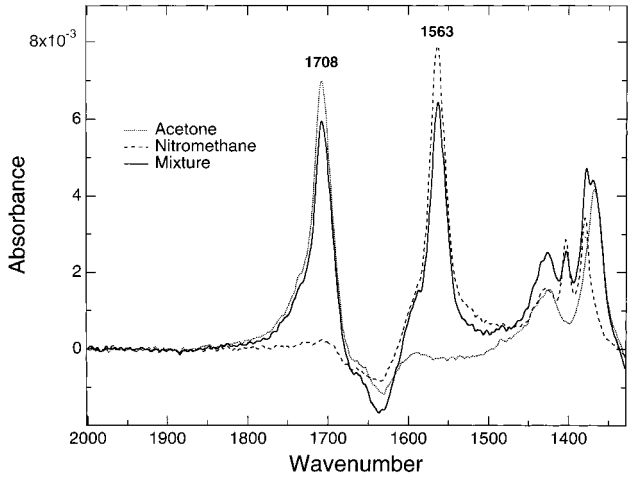

Figure 9. PM-IRRAS difference spectra for the same sample as used in Figure 8 and exposed to the same vapors: acetone (dotted), nitromethane (dashed), and a mixture of the two (solid). While competing with each other in the mixture, the acetone and nitromethane peaks decreased from their original absorbances.

humidified nitrogen ($P_{H_2O}/P_0 = 0.016$, ca. 60% relative humidity). The resulting difference spectrum for this hydration experiment was the inverse of the dehydration spectrum shown in Figure 7. Thus far, we have shown the adsorption and desorption of a single vapor, either acetone or water. Several other vapors including nitromethane, cyclohexane, methanol, pyridine, and acetonitrile were investigated; all showed reversible adsorption to these PL/SiO_2 thin films. In the following section, we expand to dosing with two vapors simultaneously.

Competitive Vapor Adsorption Experiments. To investigate competitive adsorption, an experiment was devised whereby a PL/SiO_2 thin film was exposed sequentially to acetone, nitromethane, and then a mixture of these two vapors with nitrogen purging before each new vapor. The fixed-angle in situ SPR results of this experiment are shown in Figure 8. The initial reflectivity in the presence of nitrogen gas was 37.0% *R*, and then it increased to 48.4% *R* (dotted line) upon dosing with acetone vapor ($P/P_0 = 0.016$), giving a change in reflectivity of 11.4 Δ% *R*. Purging out the acetone vapor with nitrogen caused the reflectivity to return to the baseline, and a total of four cycles were performed for each vapor to demonstrate the reversibility and reproducibility of adsorption. Next, dosing with nitromethane vapor at the same concentration ($P/P_0 = 0.016$) yielded a 10.7 Δ% *R* (dashed line), indicating a similar but slightly smaller amount of adsorption than acetone. Finally, exposure to a mixture of acetone ($P/P_0 = 0.016$) and nitromethane ($P/P_0 = 0.016$) gave an increase of 15.3 Δ% *R* or about 1.3 times as much as the individual vapors. This result is not surprising, since the total vapor concentration was doubled, and in fact, when the acetone concentration was doubled ($P/P_0 = 0.032$), the SPR signal also increased by a factor of 1.3 (data not shown). Although these SPR data in Figure 8 clearly show the amounts of adsorption and desorption in real-time, SPR measurements cannot provide direct information about how much of each different vapor is adsorbing from the mixture. For analysis of the competitive nature of adsorption occurring in the presence of vapor mixtures, we must turn to PM-IRRAS.

Figure 9 shows the three in situ PM-IRRAS difference spectra for an experiment analogous to the one described above. Rather than the four cycles performed in the SPR experiment, the sample was exposed to each vapor only once, during which a spectrum of 500 block-averaged scans was acquired, followed by 5−10 min of nitrogen purging before introducing the next vapor. The acetone spectrum (dotted line) contains peaks at 1708, 1425, and 1368 cm^{-1}. The nitromethane spectrum (dashed line) has a prominent peak at 1563 cm^{-1} as well as three smaller bands at 1428, 1404, and 1380 cm^{-1}. The solid line spectrum corresponds to adsorption from the mixture of the two vapors, and it shows all of the expected peaks from both vapors. The heights of the peaks, however, allow us to ascertain how much of each vapor is adsorbing from this mixture. Both the acetone peaks (e.g., 1708 cm^{-1}) and the nitromethane peaks (e.g., 1563 cm^{-1}) decrease in the mixture spectrum, as compared to their respective individual spectra, despite the fact that each vapor is still at its original concentration of $P/P_0 = 0.016$. Since the presence of acetone decreases the nitromethane adsorption and vice-versa, the vapors are competing for adsorption within the thin film.

The PM-IRRAS spectra allow a determination of the relative amounts of each vapor adsorbed from the mixture, and consequently, we can ascertain whether one vapor adsorbs preferentially. Upon competing with nitromethane, the acetone peak at 1708 cm^{-1} was reduced to 84 ± 2% of its original absorbance. The nitromethane peak at 1563 cm^{-1} while competing with acetone was reduced to 75 ± 7%. These values were calculated as the means and standard deviations of seven trials, and a *t*-test demonstrates that the means are statistically different at the 99% confidence level. Therefore, we conclude that the PL/SiO_2 film has a slight preference for acetone vapor over nitromethane. One would not expect an oxide such as silica to be particularly selective toward one of these vapors, but a small difference, such as we have observed, is not surprising, given all of the chromatography performed with silica stationary phases. It is impressive that PM-IRRAS was able to discern this slight difference in adsorption strength for ultrathin films exposed to a mixture of vapors.

A question remains as to whether this preference for acetone could have been predicted by experiments performed with individual vapors using a nonselective optical or mass-sensing

technique. The answer lies in the SPR data of Figure 8, which showed that acetone adsorbs slightly more strongly than nitromethane. Therefore, in this case, the PM-IRRAS results were in accord with those predicted by simple distribution constants attainable from single-vapor-dosing experiments. Nonetheless, PM-IRRAS certainly has the ability to detect any unforeseen cooperativity between vapors from a mixture.

One of our particular interests in these silica nanoparticle thin films relates to chemical sensing. As expected, the PL/SiO_2 thin films employed in this paper showed little selectivity for volatile organic compounds, as seen for acetone and nitromethane, but also for other vapors not presented here. We plan to explore some strategies for increasing selectivity such as modifying the silica nanoparticle surface with organosilanes. The multitude of these reagents opens the possibility of an array sensor having different derivatized silica nanoparticles at each spot. Since array-type sensors rely upon a pattern of adsorption across multiple elements, they do not require very high selectivity for a single vapor on any given spot. Thus, exposure of such a sensor, an "electronic nose," to a vapor mixture would likely involve competitive or cooperative adsorption between compounds. Investigation of such interactions would require PM-IRRAS, the technique put forward in this paper.

CONCLUSIONS

We have demonstrated vapor adsorption into porous ultrathin films containing silica nanoparticles and poly(L-lysine) prepared by electrostatic self-assembly from solution. In situ surface plasmon resonance measurements were employed in two modes. The more familiar angle-scanning SPR method yielded information about the absolute amount of vapor adsorbed into the film, including the estimate that acetone covered one-half of the nanoparticle surface area for a certain concentration of acetone vapor. The fixed-angle SPR method showed relative amounts of adsorption of different vapors, and it gave adsorption data in real time, which will allow future studies of kinetics. The in situ FT-IR measurements in the form of PM-IRRAS affirmed the identity of the vapor adsorbing or desorbing as well as molecular interactions occurring within the thin film.

The competitive adsorption between vapors in a mixture was explored and quantified with in situ PM-IRRAS. In this study, two compounds with strong and nonoverlapping peaks were chosen as a model case. The possibility of overlapping peaks, especially with multicomponent mixtures, may require spectral deconvolution but otherwise should present no difficulties. The good signal-to-noise ratio observed indicates applicability at lower concentrations, or with compounds that have weaker absorptions, or with nonporous ultrathin films. If necessary, the sensitivity could be increased further by employing thicker porous films, which are easily created in this case using the layer-by-layer electrostatic self-assembly approach. PM-IRRAS combines chemical-specificity, surface-selectivity, and sufficient sensitivity to qualify it as a superior technique for in situ studies of chemical vapor sensors or any other application involving vapor adsorption to thin films on metal surfaces.

ACKNOWLEDGMENT

The authors thank Bryce Nelson and Marc Anderson for the gift of the silica sol used initially in these studies. Acknowledgment is made to the donors of the Petroleum Research Fund, administered by the American Chemical Society, for support of this research.

Received for review September 11, 2001. Accepted November 29, 2001.

AC010990M